the autoxidation of polyunsaturated fatty acids (PUFA) in pulmonary macrophages,[30,31] an effect that could be due to NO_2, peroxyl, alkoxyl, and/or alkyl radicals. Nitrogen dioxide is known to add to olefinic bonds, to abstract allylic hydrogen atoms, and to initiate PUFA autoxidation.[11,12,26] Oxy radicals and alkyl radicals also can both add to unsaturated bonds and abstract allylic hydrogen atoms.[32] Autoxidation of PUFA leads to the production of malondialdehyde and other compounds that are reactive in the thiobarbituric acid (TBA) test, and malondialdehyde is known to be mutagenic.[33-35] In addition, PUFA autoxidation produces other aldehydes, particularly 4-hydroxy-2-nonenal, that are strongly cytotoxic.[36,37] Unknown factors in smoke inactivate thiol-dependent enzymes, and we have suggested that NO and NO_2 are the compounds responsible for this.[38] Peroxyl radicals can epoxidize unsaturated compounds, producing electrophilic epoxides that may be mutagenic or carcinogenic.[39,40] And finally, the oxidation of α-1-proteinase inhibitor (a1PI) is thought to be involved in the etiology of smoker's emphysema, and peroxyl radicals and other radicals in smoke may be able to affect this oxidation.[41,42] We have recently shown that our NO/air/isoprene system, like gas-phase cigarette smoke, rapidly inactivates a1PI.[43]

Acknowledgment. This work was supported by the National Institutes of Health, Grant HL-25820, and by the Council on Tobacco Research.

Registry No. PBN, 3376-24-7; PBNOx, 35822-90-3; NO, 10102-43-9; NO_2, 10102-44-0; isoprene, 78-79-5; 1,3-butadiene, 106-99-0; isobutylene, 115-11-7; propylene, 115-07-1; ethylene, 74-85-1.

(30) Lentz, P. E.; DiLuzio, N. R. *Arch. Environ. Health* **1974**, *28*, 279.
(31) Also see: Chow, C. K. *N.Y. Acad. Sci.* **1982**, *393*, 426.
(32) Pryor, W. A. "Free Radicals"; McGraw-Hill: New York, 1966.
(33) Witas, T.; Sledziewski, P. Nahrung **1980**, *24*, 243.
(34) Yau, T. M. *Mech. Ageing Dev.* **1979**, *11*, 137.
(35) Mukai, F. H.; Goldstein, B. D. *Science (Washington, D.C.)* **1976**, *191*, 868.
(36) Esterbauer, H.; Dianzani, M. V.; Schauenstein, E. In "Free Radicals, Lipid Peroxidation, and Cancer"; Slater, T. F., McBrien, D. C. H., Eds.; Academic Press: New York, 1982; pp 101–172.
(37) Schauenstein, E.; Esterbauer, H.; Zollner, H. "Aldehydes in Biological Systems"; Gore, P. H., translator; Pion Ltd.: London, 1977.
(38) Pryor, W. A.; Church, D. F.; Govindan, C. K.; Crank, G. *J. Org. Chem.* **1982**, *47*, 156.
(39) Reference 29, p 451.
(40) Marnett, L. In "Free Radicals in Biology"; Pryor, W. A., Ed.; Academic Press: New York, 1984; Vol. VI, p 64ff.
(41) Dooley, M. M.; Pryor, W. A. *Biochem. Biophys. Res. Commun.* **1982**, *106*, 981.
(42) Janoff, A.; Carp, H.; Lee, D. K.; Drew, R. T. *Science (Washington, D.C.)* **1979**, *206*, 1313.
(43) Pryor, W. A.; Dooley, M. M.; Church, D. F., to be submitted.

Photoelectron Spectra and Molecular Orbital Calculations on Bis(cyclopentadienyldicarbonylchromium, -molybdenum, and -tungsten): Nature of the Bonding of Linear Semibridging Carbonyls

Betty J. Morris-Sherwood, Cynthia B. Powell, and Michael B. Hall*

Contribution from the Department of Chemistry, Texas A&M University, College Station, Texas 77843. *Received November 14, 1983*

Abstract: The gas-phase ultraviolet photoelectron spectra are reported for the compounds $[(\eta^5\text{-}C_5H_5)M(CO)_2]_2$, where M = Cr, Mo, W. The spectra are compared to Fenske–Hall molecular orbital calculations on the chromium and molybdenum species. The 15-electron fragment, $(\eta^5\text{-}C_5H_5)M(CO)_2$, requires three additional electrons to satisfy the 18-electron rule. The fragments dimerize and the dimer can be described as a metal-to-metal triple bond with linear semibridging carbonyls. The spectra for all the dimers are similar in general appearance. The spectrum of the chromium species, however, has ionizations from the $15b_u$ and $14a_g$ orbitals that appear as distinct peaks at lower ionization energy than they do in the spectra of the molybdenum and tungsten species. These changes are a result of the nonlinear Cp–M–M framework in the chromium dimers. *The calculations suggest that the linear semibridging carbonyls are π acceptors, not π donors.* They bend over the M≡M bond in order to accept electrons from the metal–metal π bonds, but they remain linear to avoid destroying this bond. Thus, they join with the two metals to form multicenter, two-electron bonds.

Recent work shows that the species $[(\eta^5\text{-}C_5H_5)M(CO)_2]_2$, **1**, has a rich chemistry,[1-5] The molybdenum dimer reacts readily with soft nucleophiles, like phosphines, breaking the triple bond and displacing the semibridging carbonyls. Electrophiles, like iodine and hydrochloric acid, also add to the triple bond. Depending on the temperature, the iodine forms either an iodo-bridged or terminal-bound species. Mixed metal clusters such as $(\eta^5\text{-}C_5H_5)Mo(CO)_3Co(CO)_4$ and $(\eta^5\text{-}C_5H_5)(CO)_3MoMn(CO)_5$ have been formed. Other complexes formed from the molybdenum dimer include $(\eta^5\text{-}C_5H_5)_2Mo_2(CO)_4(NCNMe)_2$, $(\eta^5\text{-}C_5H_5)_2Mo_2(CO)_4(RCCR')$, and $(\eta^5\text{-}C_5H_5)_2Mo_2(CO)_4$(allene).

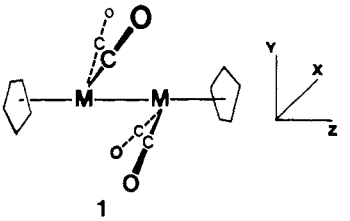

1

The fragment $CpM(CO)_2$ (Cp = $\eta^5\text{-}C_5H_5$) is a 15-electron fragment and needs three additional electrons to satisfy the 18-electron rule. Recent X-ray studies have revealed unusual structures for the series $[CpM(CO)_2]_2$ where M = Cr, Mo.[6,7]

(1) Klingler, R.; Butler, W. M.; Curtis, M. D. *J. Am. Chem. Soc.* **1975**, *97*, 3535.
(2) Bailey, W. I.; Chisholm, M. H.; Cotton, F. A.; Murillo, C. A.; Rankel, L. A. *J. Am. Chem. Soc.* **1978**, *100*, 802.
(3) Chisholm, M. H.; Cotton, F. A.; Extine, M. W.; Rankel, L. A. *J. Am. Chem. Soc.* **1978**, *100*, 807.
(4) Curtis, M. D.; Messerle, L.; Fotinos, N. A.; Gerlach, R. F. *ACS Symp. Ser.* **1981**, *155*, 221.
(5) Bailey, W. I.; Chisholm, M. H.; Cotton, F. A.; Rankel, L. A. *J. Am. Chem. Soc.* **1978**, *100*, 5764.

0002-7863/84/1506-5079$01.50/0

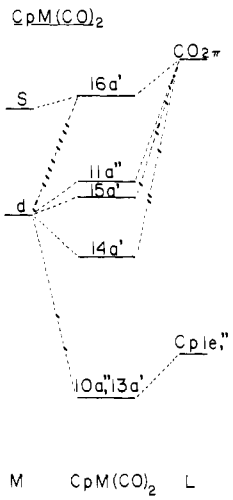

Figure 1. Molecular orbital diagram of $CpM(CO)_2$. The dashed lines indicate the principle contributions to each molecular orbital.

Both the chromium and molybdenum species have four semi-bridging carbonyls. The molybdenum species has a nearly linear M–M–Cp (center) angle while the chromium species is slightly bent. Although synthesized, the X-ray structure for the tungsten complex has yet to be reported.

Extended Hückel (EH) calculations have been reported for these complexes.[8] Although they showed significant insight into the electronic structure of this series, the calculations did not explain why the carbonyls remain linear or why the M–M–Cp angle is linear for the molybdenum species yet bent for the chromium species. The assignment of a M–M triple bond was also questioned. We have undertaken an investigation of the electronic structure of these compounds using both ultraviolet photoelectron (PE) spectroscopy and parameter-free, Fenske–Hall molecule orbital (MO) calculations.

Experimental Section

Preparation. The compounds were prepared by published procedures[9,10] and kindly supplied to us by Professor M. David Curtis.

Spectroscopy. The photoelectron spectra were taken on a Perkin-Elmer Model PS-18 photoelectron spectrometer. The argon doublet was used as an internal standard. The resolution (fwhm) was always better than 25 meV for the argon $^2P_{3/2}$ band. The temperature range for vaporization of these compounds was 90–100 °C.

Theoretical Details. The MO calculations on the chromium and molybdenum species were done on Amdahl 470 V/6 and V/7 computers using the nonempirical method of Fenske and Hall.[11] No calculation on the tungsten complex was done because of the lack of a structure determination and the lack of well-tested basis functions for third-row transition metals. The Cr(I) and Mo(I) functions were those of Richardson[12,13] with 4s, 4p exponents on Cr of 2.0 and 5s, 5p exponents on Mo of 2.2.[14] Clementi functions were used for C and O.[15] An exponent of 1.2 was used for all hydrogens. The bond lengths and angles, except where otherwise noted, were taken from the X-ray structure. The symmetry of these molecules is C_{2h} and the coordinate system has the yz plane as the plane of reflection.

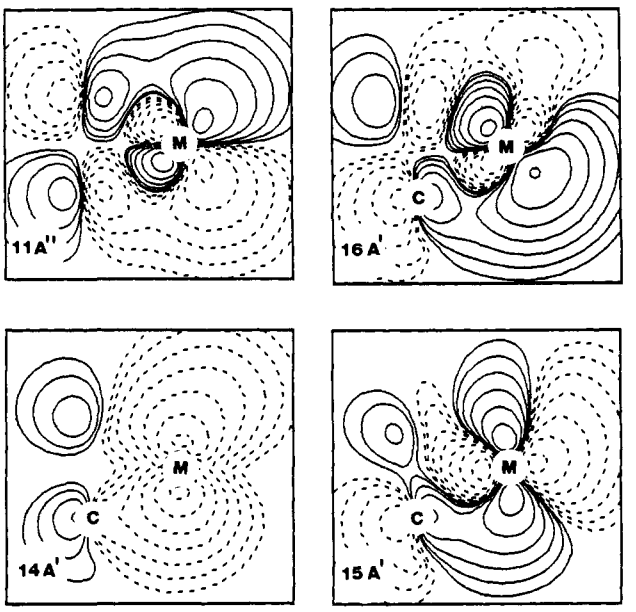

Figure 2. Contour plots for the upper valence orbitals of the fragment $CpM(CO)_2$. The fragment represented is the left half of **1**. The a′ orbitals are all plotted in the yz plane, while the a″ orbital is plotted in the xz plane (see **1**).

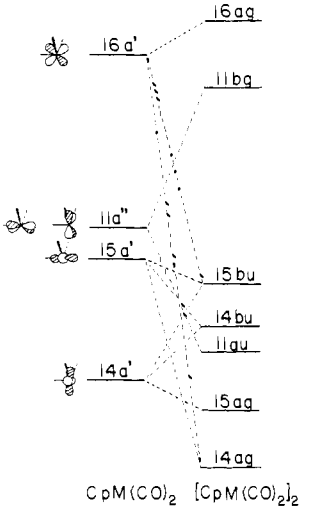

Figure 3. Molecular orbital diagram of $[CpM(CO)_2]_2$ constructed from the fragment $CpM(CO)_2$. The energy values were obtained from a Fenske–Hall calculation.

Theoretical Results

We will begin by describing the results of the Fenske–Hall MO calculations. All of the complexes have 102 valence electrons and in C_{2h} symmetry have 15 doubly occupied orbitals of b_u and a_g symmetry, 11 doubly occupied orbitals of a_u symmetry, and 10 doubly occupied orbitals of b_g symmetry. We will describe the formation of these molecules in terms of their $[CpM(CO)_2]$ fragments. The local coordinate system is shown in **1**.

The molecular orbital diagram for the fragment $[CpM(CO)_2]$ is shown in Figure 1. Only the upper valence levels are shown; these should correspond to the orbitals involved in dimer formation. The lowest unoccupied molecular orbital (LUMO), 16a′, is characterized by an antibonding combination between the metal d_{yz} orbital and the cyclopentadiene $1e_1''$. It also contains significant metal s character. The highest occupied molecular orbital (HOMO), 11a″, is only singly occupied and is bonding between the metal d_{xy} and d_{xz} and the carbonyl 2π orbitals. The 15a′ orbital is mainly the bonding interaction between the metal d_{z^2} and the

(6) Curtis, M. D.; Butler, W. M. *J. Organomet. Chem.* **1978**, *155*, 131.
(7) Klingler, R. J.; Butler, W. M.; Curtis, M. D. *J. Am. Chem. Soc.* **1978**, *100*, 5034.
(8) Jemmis, E. D.; Pinhas, A. R.; Hoffmann, R. *J. Am. Chem. Soc.* **1980**, *102*, 2576.
(9) (a) Hackett, D.; O'Neill, P. S.; Manning, A. R. *J. Chem. Soc., Dalton Trans.* **1974**, 1625. (b) Ginley, D. W.; Bock, D. R.; Wrighton, M. S. *Inorg. Chim. Acta* **1977**, *23*, 85.
(10) Curtis, M. D.; Fotinos, N. A.; Messerle, L.; Sattelberger, A. P. *Inorg. Chem.* **1983**, *22*, 1559.
(11) Hall, M. B.; Fenske, R. F. *Inorg. Chem.* **1972**, *11*, 768.
(12) Richardson, J. W.; Nieuwpoort, W. C.; Powell, R. R.; Edgell, W. F. *J. Chem. Phys.* **1962**, *36*, 1057.
(13) Richardson, J. W.; Blackman, M. J.; Ranochak, J. E. *J. Chem. Phys.* **1973**, *58*, 3010.
(14) Barber, M.; Conner, J. A.; Guest, M. F.; Hall, M. B.; Hillier, I. H.; Meredith, W. N. E. *J. Chem. Soc., Faraday Trans. 2* **1972**, *54*, 219.
(15) "Tables of Atomic Functions", a supplement to a paper by: Clementi, E. *IBM J. Res. Dev.* **1965**, *9*, 2.

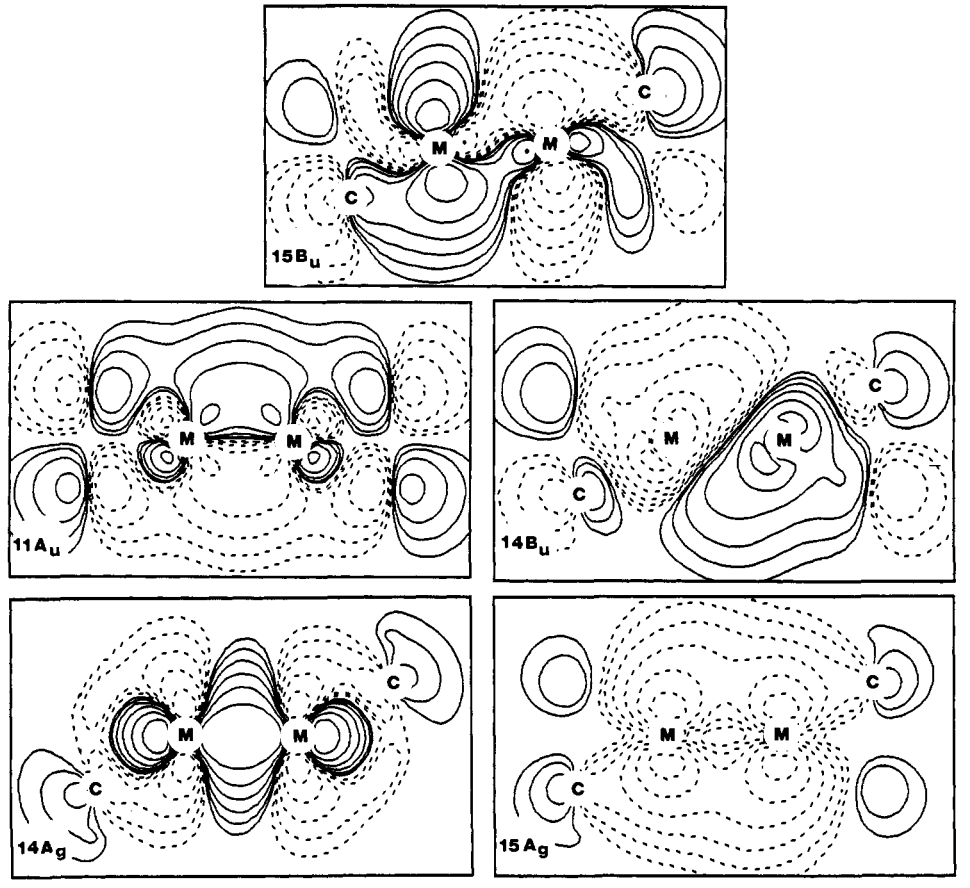

Figure 4. Contour plots for the upper valence orbitals of the dimer $[CpM(CO)_2]_2$. The a_g and b_u orbitals are plotted in the *yz* plane, while the a_u orbital is plotted in the *xz* plane (see **1**).

carbonyl 2π orbitals. In the 14a′ orbital, the main interaction is a bonding one between the $d_{x^2-y^2}$ orbital on the metal and the carbonyl 2π orbital. The next two orbitals, the 10a″ and 13a′, are degenerate and contain a large amount of Cp $1e_1''$ character and form the major component of the Cp to metal bond with the metal d_{xz} and d_{yz} orbitals.

Contour plots of the metal-based orbitals are shown in Figure 2. The 16a′ orbital is tipped away from the carbonyls and is both σ and π with respect to the metal–metal direction. The 15a′ orbital, which is primarily σ-like, is tipped between the carbonyls. Because of the arrangement of the two fragments the 15a′ orbital of one fragment points toward the 16a′ orbital of the other. With respect to the M–M direction the 11a″ orbital is both δ and π in character, while the 14a′ is primarily δ in character.

Figure 3 shows the result of bringing two of these fragments together to form the dimer, $[CpM(CO)_2]_2$. To the left of the fragment's eigenvalue a pictoral representation is shown of the main metal d contribution. The lines emanating from the d orbital lobes represent the approximate position of Cp ring, to the left of the metal, and the two carbonyls, above the metal. The unoccupied $16a_g$ orbital has contributions mainly from the fragments 16a′ and 17a′. The LUMO, $11b_g$, is characterized mainly by contributions from the 11a″ and 12a″ orbitals of the fragment. The $15b_u$ orbital is the HOMO of the dimer and is primarily composed of 14a′ and 15a′ with some 16a′. Although both the 14a′–14a′ interaction and the 15a′–16a′ interaction are antibonding in the $15b_u$ orbital this orbital has a bonding 15a′–16a′ interaction. The $11a_u$ orbital is mainly characterized by a bonding π interaction and an antibonding δ interaction, which is dominated by the 11a″ orbital of the fragment. The $15a_g$ and $14b_u$ orbitals are metal δ bonding and antibonding combinations, respectively, which result primarily from the 14a′ orbital of the fragment. The $14b_u$ orbital also has a small contribution from the 15a′ orbital. The $14a_g$ orbital is composed of bonding 15a′–15a′ and 15a′–16a′ interactions. However, most of the net 15a′–15a′ bonding contribution is cancelled by antibonding contributions in the $14b_u$ and $15b_u$ orbitals. The next four orbitals, $10b_g$, $13a_g$, $10a_u$, and $13b_u$, all contain a large amount of Cp $1e_1''$ character and form the major component of the Cp to metal bond. At still lower energy are the 5σ CO to metal bonds, $9b_g$, $9a_u$, $12b_u$, and $12a_g$.

Figure 4 contains contour plots of the upper valence orbitals which contain important dimer interactions. By comparing the fragment plots for the 15a′ and 16a′ orbitals with the molecule plot for the $15b_u$ (HOMO) orbital, one clearly sees the formation of the latter orbital from a bonding combination of these two fragment orbitals. The $14b_u$ and $14a_g$ orbitals are the antibonding and bonding combinations of the 14a′ fragment orbitals. The π bonding orbital, $11a_u$, is composed almost entirely from the 11a″ orbital. The σ bond in the $14a_g$ orbital is partly canceled by antibonding σ terms in the $14b_u$ and $15b_u$ orbitals. The simplest view would relegate the $14b_u$ and $15a_g$ orbitals to δ-like lone pairs, the $14a_g$ orbital to the σ bond, and the $11a_u$ and $15b_u$ orbitals to the π bonds. However, the σ and π interactions in the $14a_g$ and $15b_u$ orbitals can also be viewed as two localized "banana" bonds. In this description the electron pair in the 15a′ orbital of one fragment forms a bond with the 16a′ orbital of the other fragment to produce one of these two "banana" bonds. The other "banana" bond is formed by reversing the fragments. These bonds extend between the carbonyls above the below the M–M axis (see **1**).

We have examined two distortions of the idealized geometry shown in **1**. In the first of these the O atoms of the carbonyl groups are rotated about the C atoms until the C → O vectors are perpendicular to the M–M axis (**2**). The four carbonyls are now

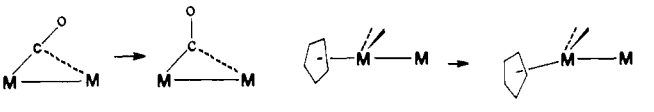

2 3

much closer to a "normal" semibridging geometry. This motion destroys a large fraction of the M–M π bonding but does not affect the σ bonding. In the second distortion the Cp rings are tipped

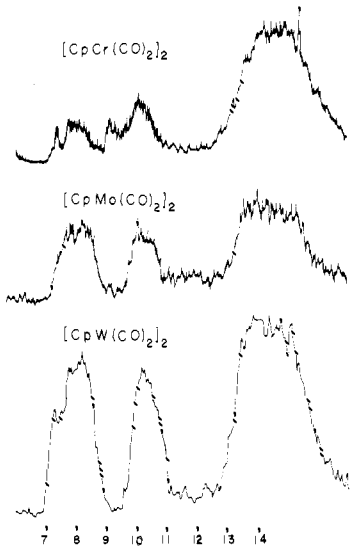

Figure 5. Photoelectron spectra of the $[CpM(CO)_2]_2$ complexes (M = Cr, Mo, W).

"back", away from the carbonyls (**3**). The resulting geometry is close to that found for the chromium derivative. The effect of this bend on the metal–metal orbitals is to stabilize slightly the $15b_u$ (HOMO) orbital to stabilize strongly the $14b_u$ and $11a_u$ orbitals, and to destabilize the $15a_g$ and $14a_g$ orbitals. Similar changes were predicted by the EH calculations.[8] Overall, these changes narrow the energy gap between highest and lowest energy occupied metal orbitals. The calculations do not offer a clear-cut reason why this bend occurs in the Cr derivative. For example, the bend has an overall destabilizing effect on the five metal levels, which is completely canceled by a stabilizing effect on the four Cp levels. However, the bend does decrease the steric repulsion between the CO's and Cp ring on the same metal. This steric repulsion would be most important for the smallest metal atom, chromium.

Spectroscopic Results

The spectra of the complexes $[CpM(CO)_2]_2$ (M = Cr, Mo, W) are shown in Figure 5. In all the spectra there exists in the region above 12.5 eV a large, very broad band. The lack of fine structure in this band is typical of bands with a number of close, overlapping ionizations. The ionizations of the Cp $3e_1'$ (the C–H σ bonds), the Cp $3e_2'$ (the C–C σ bonds), the Cp $1a_2''$ (the C–C π bond), the CO 5σ, and the CO 1π orbitals are assumed to be within this region. The IE for the lower energy bands and their assignments, which are made below, are collected in Table I.

$[CpCr(CO)_2]_2$. The first ionization in the spectrum is a narrow band at 7.25 eV on the left-hand side of a broader band. This narrow band corresponds to ionization from the HOMO, $15b_u$, which in the geometry with nonlinear Cp's is a chromium δ^* orbital. There is a distinct but poorly resolved splitting at 7.66 and 7.98 eV in the next band. This band is taken to be three ionizations and is assigned to be the next three occupied orbitals, $15a_g$ at 7.66 eV and the $14b_u$ and $11a_u$ at 7.98 eV. The ionization at 8.80 eV is assigned to the $14a_g$ orbital. The band at 9.6 eV shows the typical asymmetry of a cyclopentadienyl ionization[16] and is thus assigned to the $10b_g$, $13a_g$, $10a_u$, and $13b_u$ orbitals.

$[CpMo(CO)_2]_2$. Here the first band is split into two distinct peaks, the first at 7.58 eV is assigned to the $15b_u$ and $14b_u$ orbitals. This band is slightly unsymmetrical, and the $15b_u$ ionization is probably responsible for the shoulder on the low-energy side of this band at approximately 7.35 eV. The band at 8.13 eV has similar intensity and width as the band at 7.58 eV, and its is therefore assumed that this band is the result of two ionizations, the $11a_u$ and the $15a_g$. The band at 9.83 eV does not appear to have the typical shape of a cyclopentadienyl band because the ionization from the Mo–Mo σ orbital, $14a_g$, is also within the region of ionizations from the $10b_g$, $13a_g$, $10a_u$, and $13b_u$ orbitals.

$[CpW(CO)_2]_2$. The first band has a wide shoulder on its left side at 7.36 eV. Ionization from the $15b_u$ orbital is assigned to this shoulder. The next band is more intense than the first, and it is assumed that the $14b_u$ orbital is on the low-energy side of this band at 7.83 eV with ionizations from the $11a_u$ and the $15a_g$ orbitals being located at 8.18 eV. The band at 10.0 eV is assigned to the $14a_g$ ionization and the Cp $1e_1''$ ionizations, the $10b_g$, $13a_g$, $10a_u$, and $13b_u$ orbitals.

Some peaks in the spectra were assigned on the basis that certain types of ionizations are not expected to show much dependence on whether M is Cr, Mo, or W.[17] In the spectra of all these compounds, the ionizations from Cp occur at similar energies, 9.60, 9.83, and 10.00 eV, but are stabilized more by the heavier metal. The $15a_g$ and $14b_u$ orbitals with some carbonyl 2π and M–M δ character also remain at approximately the same energy in all three spectra. This is in contrast to an orbital such as $14a_g$, an orbital with strong M–M σ bonding character, which is expected to increase in IE as the metal descends the periodic table. Ionizations from this orbital occur, from Cr to Mo to W, respectively, at 8.80, 9.83, and 10.00 eV. The relative order of the $11a_u$ and $14b_u$ orbitals was assigned on the basis of our calculations reported here. However, this order is very sensitive to small changes in the basis functions and geometry and could be reversed in some or all of the spectra. Also, we have not accounted for spin–orbit coupling, which will mix the ion states of the W dimer.

Table I. Ionization Energies and Assignments for $[CpM(CO)_2]_2$

M	energy, eV	assignment
Cr	7.25	$15b_u$
	7.66	$15a_g$
	7.98	$14b_u$, $11a_u$
	8.80	$14a_g$
	9.60	$10b_g$, $13a_g$, $10a_u$, $13b_u$
Mo	7.35	$15b_u$
	7.58	$14b_u$
	8.13	$11a_u$, $15a_g$
	9.83	$14a_g$, $10b_g$, $13a_g$, $10a_u$, $13b_u$
W	7.36	$15b_u$
	7.83	$14b_u$
	8.18	$11a_u$, $15a_g$
	10.00	$14a_g$, $10b_g$, $13a_g$, $10a_u$, $13b_u$

Discussion

Extended Hückel calculations[8] on $[CpM(CO)_2]_2$ showed a Mulliken overlap population between M and distal C(CO) to be approximately a third (0.28) of that between M and directly bound C(CO). Although the Fenske–Hall MO calculations show a smaller ratio (0.10), it is still large enough to indicate a semibridging interaction. To our surprise, there is no donation from the CO 1π orbitals to the metal. In fact, the calculations show that in the distal carbonyl–metal interaction the carbonyl actually accepts electrons from the metal. Similar effects were seen in the (EH) calculations.[8] If this distal interaction is an acceptor interaction rather than a donor interaction,[7] the general description of these systems needs modification.

Compounds which have a linear, semibridging carbonyl are usually unsaturated; i.e., if all carbonyls were terminal the molecule would need multiple M–M bonds to satisfy the 18-electron rule. Compounds which have bent, bridging or semibridging, carbonyls are generally saturated and need only a single M–M bond to satisfy the 18-electron rule. Thus, when a carbonyl bends over in a saturated system, it points its π acceptor orbital at the other metal since it is accepting electron density from one of the "nonbonding" electron pairs on the other metal. When a carbonyl bends over in an unsaturated system, it points its π acceptor orbital at the midpoint of the metal–metal bond. In the latter case the carbonyl is participating in a three-center, two-electron bond, and bending

(16) Lichtenberger, D. L.; Fenske, R. F. *J. Am Chem. Soc.* **1976**, *98*, 50.

(17) Morris-Sherwood, B. J.; Kolthammer, B. W. S.; Hall, M. B. *Inorg. Chem.* **1981**, *20*, 2771.

the carbonyl would interrupt this interaction.

As a very simple example, let us consider two metals each with an orbital appropriate for π bonding and a single carbonyl group with a π acceptor orbital. We will represent the π orbital on each metal by only one lobe, **4**, and the carbonyl π acceptor orbital by a p orbital on carbon, **5**. In a saturated M-M system both

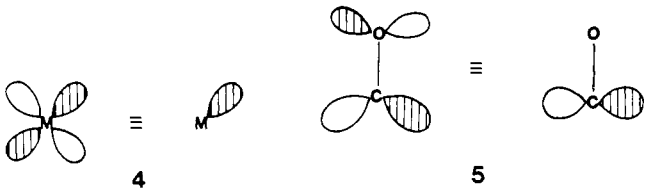

4 **5**

6 **7**

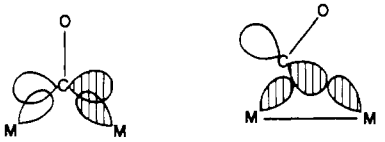

8 **9**

the symmetric combination of metal π orbitals, **6**, and the antisymmetric combination, **7**, are occupied. A carbonyl group will achieve maximum interaction with this system by orienting itself perpendicular to the M-M bond axis so that its π acceptor orbital interacts with the antisymmetric combination, **7**. The resulting occupied orbitals will then be **6** and **8**. In an unsaturated M-M system only the symmetric combination, **5**, will be occupied. In order to stabilize this system the carbonyl group will turn to present only one lobe of the π acceptor orbital to the metals, forming a three-center, two-electron bond. In this case only the 3-c, 2-e bond, **9**, is occupied. Our results also explain the nature of the bonding found in metal carbonyl fragments bonding to Lewis acids.[18] Here, the linear semibridging CO is interacting with the occupied dative (d_π metal $\rightarrow$ p_π acid) MO, while the corresponding antibonding combination is empty. Recently, Bênard, Dedieu, and Nakamura have suggested a similar model to explain the linear, semibridging carbonyl in $Mn_2(CO)_5(dppm)_2$.[19]

The calculations do not completely explain why the M-M-Cp angle is linear when M = Mo but bent 15° when M = Cr. For a fixed $M_2(CO)_4$ (M = Cr, Mo) fragment, contacts between the ring and the carbonyls are decreased as the cyclopentadiene ring is bent. The larger molybdenum atoms allow this distance to increase so that steric crowding does not influence the bonding and structure in the molybdenum species. The 15° Cr-Cr-Cp bend is a minor structural change in order to accomodate these nonbonding repulsions. Although this may not be the only reason for the bend, it is the only one offered by our calculations.

With the above explanation in mind, the ionizations at 7.25 and 8.80 eV in the spectrum of the chromium species can be readily explained. These bands were assigned as ionizations from the $15b_u$ and $14a_g$ orbitals, respectively. As the distortion to a nonlinear M-M-Cr angle occurs the $14a_g$ orbital becomes less stable, and its ionization now appears before the Cp ionizations. The $11a_u$ and $14b_u$ orbitals are stabilized, which isolates the $15b_u$ orbital and it appears well separated from the other M ionizations. These results support the idea that the series $[CpM(CO)_2]_2$ would prefer a linear M-M-Cp angle and that as this angle is decreased the $15b_u$ and $14a_g$ orbitals reflect this relative destabilization and move to lower IE.

Acknowledgment. We gratefully acknowledge the support of the Robert A. Welch Foundation (Grant No. A-648) and the National Science Foundation (Grant No. CHE79-20993 and CHE83-09936) as well as the gift of the compounds from Professor M. David Curtis (University of Michigan).

(18) Curtis, M. D.; Han, K. R.; Butler, W. M. *Inorg. Chem.* **1980**, *19*, 2096 and references therein.
(19) Bênard, M.; Dedieu, A.; Nakamura, S. *Nouv. J. Chim.* **1984**, *8*, 149.

Electron-Transfer Fluorescence Quenching of Radical Ions. Experimental Work and Theoretical Calculations

Jens Eriksen,* Karl Anker Jørgensen,* Jan Linderberg, and Henning Lund

Contribution from the Department of Chemistry, University of Aarhus, DK-8000 Aarhus C, Denmark. *Received December 29, 1983*

Abstract: The fluorescence of the anthraquinone radical anion and the thianthrene radical cation is quenched via an electron-transfer mechanism by added electron acceptors and donors, respectively. The quenching data are treated in terms of the Marcus theory leading to very large reorganization energies, ΔG^*_0 (10.0 and 15.3 kcal/mol for the two radical ions). Apparently the Weller equation is less suited for treatment of the fluorescence data in these systems. The large reorganization energies are analyzed by theoretical calculations based mainly on the energy weighted maximum overlap (EWMO) model. According to these calculations the photochemically excited anthraquinone radical anion is folded into a geometry quite different from the planar ground state of anthraquinone thus resulting in a prediction of a large bond reorganization energy.

Electron-transfer fluorescence quenching continues as an active field of study among photochemists and photophysicists.[1-4] Most work in this field has been centered around electron transfer to or from the singlet excited state of fluorescing aromatic molecules

(1) Rehm, D.; Weller A. *Isr. J. Chem.* **1970**, *8*, 259.
(2) (a) Eriksen, J.; Foote, C. S. *J. Am. Chem. Soc.* **1980**, *102*, 6083. (b) Eriksen, J.; Plith, P. E. *Tetrahedron Lett.* **1982** *23*, 481.
(3) Maroulis, A. J.; Shigemitsu, Y.; Arnold, D. R. *J. Am. Chem. Soc.* **1978** *100*, 535 and references cited therein. Brown-Wensley, K. A.; Mattes, S. L.; Farid, S. *J. Am. Chem. Soc.* **1978**, *100*, 4162.

0002-7863/84/1506-5083$01.50/0